A COMPUTER PROGRAM FOR THE DESIGN OF OPTIMUM CATALYTIC MONOLITHS FOR CO_2 LASERS

K. Guinn, S. Goldblum, E. Noskowski, and R. Herz*
Chemical Engineering Group, Mail Code B-010
University of California, San Diego
La Jolla, California

INTRODUCTION

Pulsed CO_2 lasers have many applications in aeronautics, space research, weather monitoring and other areas. Full exploitation of the potential of these lasers is hampered by the dissociation of CO_2 that occurs during laser operation. The development of closed-cycle CO_2 lasers requires active CO-O_2 recombination (CO oxidation) catalysts and design methods for implementation of catalysts inside lasers. This paper will discuss the performance criteria and constraints involved in the design of catalyst configurations for use in a closed-cycle laser and will present several design studies performed with a computerized design program that we have written. Trade-offs between catalyst activity and dimensions, flow channel dimensions, pressure drop, O_2 conversion and other variables will be discussed.

A pulsed CO_2 laser produces useful laser light output when the laser gas volume is exposed to a high electrical potential for a period on the order of milliseconds [1,2]. Low lying vibrational-rotational energy level CO_2 molecules are excited to higher energy levels. The relaxation of the excited molecules to low lying energy levels produces infrared radiation ($\approx 10\mu m$). The energy deposited by the electrical discharge alters the composition of the gas mixture by dissociation of CO_2 into stoichiometric ratios of CO and O_2. In a high pulse repetition rate (PRR) CO_2 laser system, without a method of recombining the CO and O_2, the laser gas O_2 concentration would continue to increase with time. Depending on the particular system used, O_2 concentrations above a threshold level, on the order of 1%, severely degrade the laser output quality. The lasing process also raises the temperature of the laser gas volume. The output of the laser is sensitive to the temperature of the operating gas due to the effect of temperature on the distribution of CO_2 molecules among the rotational-vibrational energy levels.

An open-cycle laser system requires a continuous supply of fresh gas to maintain O_2 concentrations below threshold levels. The higher the PRR, the higher the fresh gas flow rate required to maintain acceptable O_2 concentrations. If rare isotope CO_2 gases [1,3], such as $^{12}C^{18}O_2$, were to be used in an open-cycle laser system, the cost of supplying large quantities of CO_2 gases would be prohibitive. The safety requirements for handling and for the disposal of CO, O_2, and CO_2 gases is another concern for open-cycle systems. Clearly, for portable uses, such as in satellites or in the field, open-cycle system operation is not feasible.

*Author to whom correspondence should be addressed.

Closed-cycle systems can be envisioned to require a one time charge of the operating gas and to operate for a given number of pulses (>10^7) at a specified PRR and power output [4-7]. Portable closed-cycle systems would necessarily have power consumption constraints and, therefore, be limited in the output power and PRR. In a typical closed-cycle CO_2 laser system (Fig. 1), a gas mixture, comprised of CO_2 and other "inert" gases, is continuously recirculated through the system by a blower. The recombination of CO and O_2 is accomplished by the monolith catalyst section of the system (Fig. 2) and provides the laser section with a fresh supply of operating gas. The heat exchangers allow for the operation of the monolith catalyst section at elevated temperatures while maintaining moderate laser section temperatures. The monolith catalyst material is very porous (high surface area) and has catalytic material dispersed throughout. The performance of the monolith catalyst is measured by the section's ability to recombine CO and O_2, the size and weight of the monolith, and the pressure drop produced as a result of gas flow through the monolith. Monolith catalyst performance is dependent on a number of interrelated factors, such as the catalyst's geometry, convective heat and mass transport rates from the bulk gas to the catalyst, inlet gas properties, inlet molar gas flow rate, and catalytic activity. A monolith support is chosen over other supports, e.g. powders, beads, etc., because of the reduced level of particulate production, and the sturdiness of the monolith under high volumetric gas flow conditions.

MONOLITH CATALYST SECTION MODEL

A flexible model of the monolith catalyst may be developed to determine the bulk-average gas temperature, composition, and pressure along the length of the monolith. The adjustable parameters required to specify the operating condition of the monolith are listed in Table 1. The model assumptions, balance equations, and model results follow.

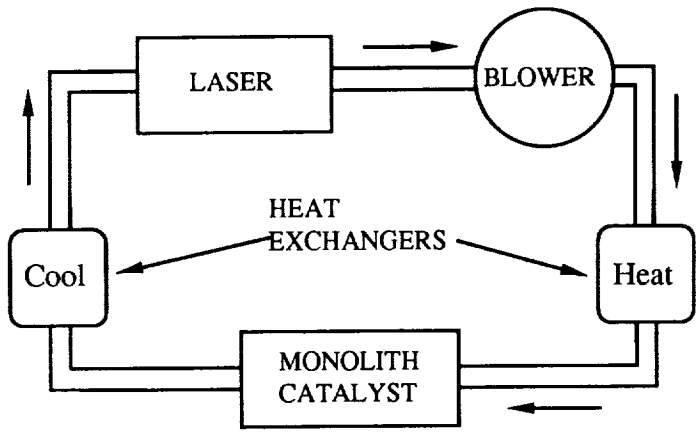

Figure 1. A typical closed-cycle CO_2 laser.

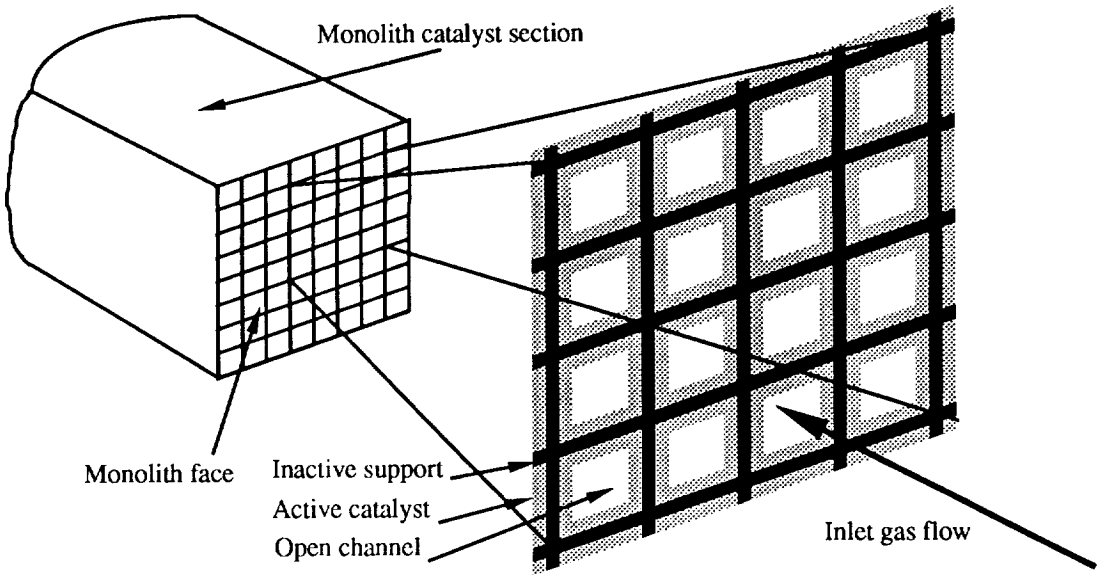

Figure 2. Monolith catalyst section.

Model Assumptions

- Steady state conditions.
- Identical conditions exist in each channel of the monolith.
- Channel gas flow is laminar and fully developed. The neglect of entrance effects for heat and mass transfer calculations provide for a conservative estimate of the amount of catalyst required. Pressure drop due to entrance and exit effects is neglected; therefore, the actual pressure drops will be somewhat greater than calculated.
- The kinetics of the reaction, $^1/_2O_2 + CO \rightarrow CO_2$, is first-order overall. That is, the reaction rate is $\propto [O_2]^{a} [CO]^{b}$, where the sum of a and b equals one. O_2 and CO_2 appear in stoichiometric ratios, $2:1 \equiv CO:O_2$. The concentration of O_2 is followed and the remaining species concentrations are calculated. The effect of temperature on the reaction rate is through an Arrhenius dependence of a reaction rate constant.
- Inlet gas composition, temperature and flow rate are known. Gas properties, viscosity, diffusivity, and thermal conductivity, are updated with changes in temperature, pressure, and reactant concentrations.
- Diffusivity in the porous catalytic layer is calculated using size and void fraction of micropores and macropores. Equimolar counterdiffusion in porous catalytic layer is assumed.
- Either adiabatic or isothermal monolith operating conditions can be selected by the operator. These two operating conditions provide the upper and lower bounds for oxygen conversion for a given inlet gas condition.
- Axial heat conduction in the porous catalytic layer and support is assumed to be negligible. For adiabatic monolith operation, transverse heat conduction in the porous catalytic layer and support is assumed to be such that the porous catalytic layer and support temperature are uniform transversely.

- Slab geometry is used for calculation of the species concentration in the porous catalytic layer. A characteristic porous catalytic layer thickness is calculated to account for porous catalytic material in the channel corners.
- Heat and mass transport between the flowing gas and the channel walls are described using the limiting Sherwood (Sh_∞) and Nusselt (Nu_∞) numbers for constant wall concentration and temperature boundary conditions in square channels [8].

Model balance equations

The steady state conservation equations for O_2 in the flowing gas and O_2 in the porous catalytic layer are

$$\frac{d\Phi_G}{d\zeta} = -\frac{\gamma}{\Gamma}\left[\Phi_G - \Phi_W\right] \quad , \text{and} \quad \frac{d^2\Psi}{d\lambda^2} = \varphi^2\Psi \quad , \tag{1,2}$$

with initial and boundary conditions,

$$\Phi_G = 1 \text{ at } \zeta = 0 \quad , \quad \Psi = 1 \text{ at } \lambda = 0 \text{ for all } \zeta \quad , \text{and} \quad \frac{d\Psi}{d\lambda} = 0 \text{ at } \lambda = 1 \quad . \tag{3,4,5}$$

Φ_G is the dimensionless bulk-average O_2 molar flow rate in the flowing gas. Variables and parameters are defined in detail in the notation list. Φ_W is the O_2 concentration at the channel wall times bulk-average volumetric flow rate divided by the inlet bulk-average O_2 molar flow rate. [$\Phi_G - \Phi_W$] is proportional to the concentration driving force for transport of O_2 from the flowing gas to the channel wall. ζ is the dimensionless distance down the length of the monolith. Ψ is the dimensionless O_2 concentration inside the porous catalytic layer at a dimensionless depth λ into the layer. The solution to Eqn. 2 yields an overall O_2 reaction rate in the porous catalytic layer as a function of Φ_W. At steady state, this reaction rate is equal to the rate of transport of O_2 from the flowing gas to the channel wall, and leads to

$$\Phi_W = \Phi_G\left[\frac{1}{\alpha + 1}\right] \quad . \tag{6}$$

The steady state energy balance on the flowing gas relates the rise in the dimensionless bulk-average temperature of the flowing gas, θ_G, to the heat transferred to the gas from the channel wall and yields

$$\frac{d\theta_G}{d\zeta} = -\left[\frac{d_h\, S\, St}{\Gamma}\right]\left[\theta_G - \theta_W\right] \quad , \text{ with initial condition,} \quad \theta_G = 1 \text{ at } \zeta = 0 \quad , \tag{7,8}$$

where θ_G is the dimensionless bulk-average temperature of the flowing gas, and θ_W is the dimensionless temperature at the channel wall. An energy balance on the porous catalytic layer equates the heat generation from the oxygen consumption reaction to the heat transferred from the porous catalytic layer and yields

$$-\left[\frac{\omega\,\alpha}{\Gamma}\right]\Phi_W = \left[\theta_G - \theta_W\right] \quad . \tag{9}$$

Combining the two energy balance equations, Eqns. 7 and 9, and substituting for Φ_W using Eqn. 6 results in two final differential equations to be integrated,

$$\frac{d\Phi_G}{d\zeta} = -\left[\frac{\Gamma}{\gamma} + \frac{\Gamma}{\alpha\gamma}\right]^{-1}\Phi_G \quad , \text{and} \quad \frac{d\theta_G}{d\zeta} = \frac{[d_h\,S\,\alpha\,\omega\,St]}{[\,1+\alpha]\,\Gamma^2}\,\Phi_G \quad , \tag{10,11}$$

with the same initial conditions for Φ_G and θ_G as above. Pressure drop for the laminar flow is calculated using the Hagen-Poiseuille equation,

$$\frac{d\wp}{d\zeta} = \frac{-32}{Eu\,Re} \quad , \text{with an initial condition of} \quad \wp = 1 \quad \text{at} \quad \zeta = 0 \quad , \tag{12,13}$$

where $\wp$ is the dimensionless pressure. Eqns. 10-12 are coupled to each other through the variable Φ_G and the parameters α, ω, Γ, γ, St, Eu, and Re, each of which is a function of θ_G, Φ_G and $\wp$.

Model results

The adjustable parameters required to specify the monolith catalyst section operating conditions are listed below in Table 1. They are used to compute the dimensionless parameters α, ω, Γ, γ, St, Eu, and Re, and to integrate the dimensionless variables in Eqns. 10-12. A computer program was written to perform integration using the fourth-order Runge-Kutta method. The program allows θ_G, θ_W, Φ_G, Φ_W and $\wp$ to be determined as ζ varies from zero to the desired dimensionless monolith catalyst section length. The computer program requires readily available parameters to calculate parameters such as mass and heat transfer coefficients, bulk-gas and effective diffusion coefficients, and thermal conductivity. Results for a monolith catalyst section operating under conditions specified in Table 1 are shown in Figs. 3, 4 and 5.

Fig. 3 shows the behavior of θ, Φ, and $\wp$ as ζ varies from 0 to 100. $\theta_G \approx \theta_W$ and $\Phi_G \approx \Phi_W$; therefore, θ_G, θ_W, Φ_G, and Φ_W are not shown individually on this small scale plot. The behavior of θ, Φ, and $\wp$ can be explained using Eqns. 1-12, in which all parameters and variables are positive valued. The right side of equation (11) is positive, therefore, $d\theta_G/d\zeta > 0$. The left hand side of Eqn. 9 is negative, therefore, $\theta_W > \theta_G$. Similar examination of Eqns. 6 and 10 results in $d\Phi_G/d\zeta < 0$ and $\Phi_W > \Phi_G$. Eqn. 12 indicates that $d\wp/d\zeta < 0$. The drop in $\wp$ is negligible for the gas flow rate specified in Table 1. Pressure drop can be significant for higher gas flow rates.

Fig. 4 is an expansion of Fig. 3 in the ζ = 45 to 50 region. The separation between θ_G and θ_W is now visible and provides an indication of the thermal driving force between the channel wall and the bulk-gas. Heat produced from the oxidation of CO in the active catalyst layer of the channel wall is transferred from the channel wall to the bulk-gas.

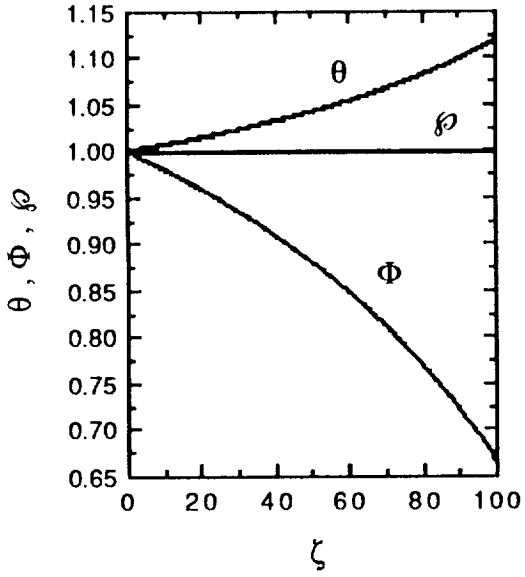

Figure 3. Results for Table 1 case. Dimensionless bulk-gas temp (θ), pressure (℘), and O_2 concentration (Φ) vs distance from mono-inlet (ζ).

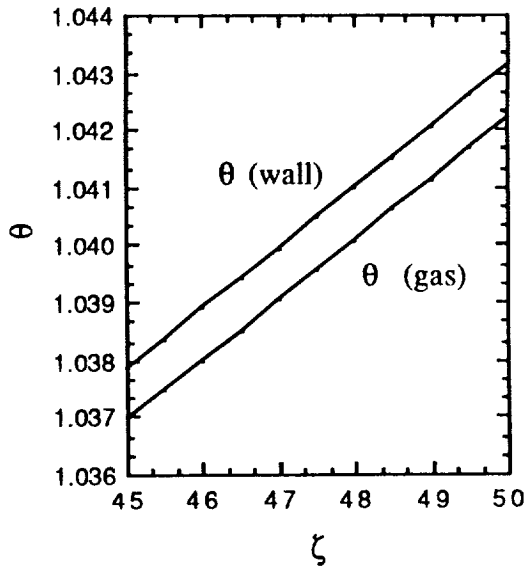

Figure 4. Dimensionless temperatures for Table 1 case.

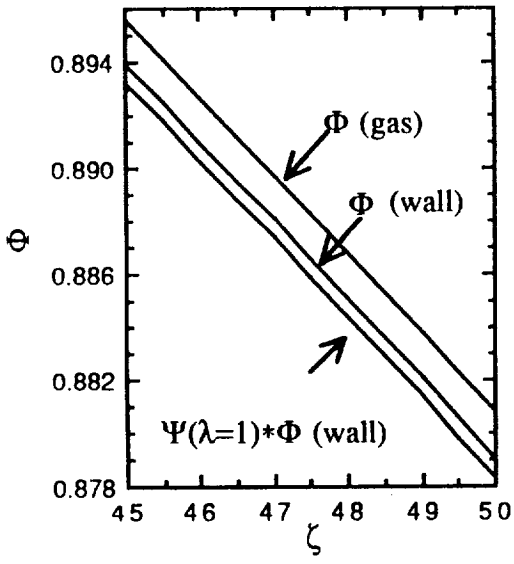

Figure 5. Dimensionless O_2 concentrations for Table 1 case.

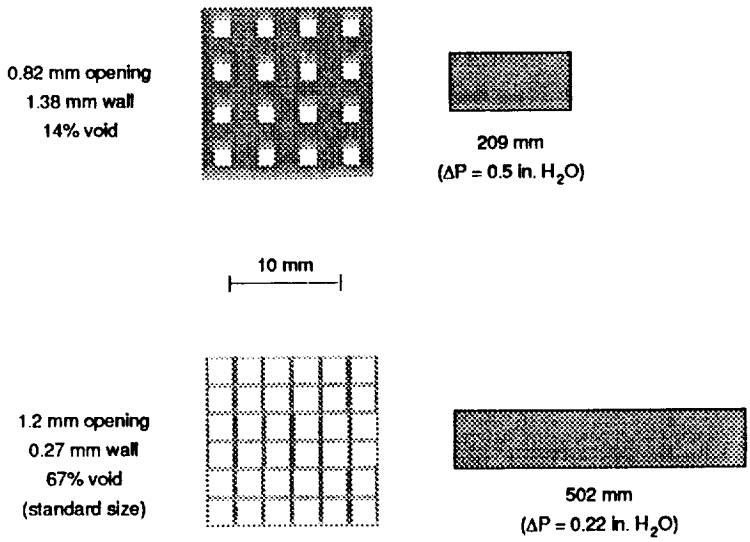

Figure 6. Optimum design vs. standard commercial size.

Fig. 5 is an expansion of Fig. 3 in the ζ = 45 to 50 region. An additional curve, $\Psi(\lambda=1)*\Phi_W$, is the scaled O_2 concentration at the centerline of the monolith channel support wall. O_2 is consumed in the porous catalytic layer as mass transport to the center of the monolith channel support wall occurs, therefore $\Psi(\lambda=1)*\Phi_W$ is less than Φ_W or Φ_G. The separation between the curves indicates the O_2 mass transport driving force. The difference between Φ_G and Φ_W is an indication of the driving force between the bulk gas and the channel wall. The difference between Φ_W and $\Psi(\lambda=1)*\Phi_W$ is an indication of the driving force between the channel wall and the centerline of the monolith channel support wall.

Table 1: Monolith catalyst section operating parameters

Monolith dimension

Facial cross sectional area = 1.0e+4 mm^2
Support + active layer thickness = 1mm
Active layer thickness = 0.25mm

Gas inlet properties

Flowrate = 0.25 liters/s
Temperature = 300 K
Pressure = 101.325 kPa
Composition 37% CO_2, 2% CO, 1% O_2, 40% N_2, 20% He

Thermal operation is "adiabatic"

Catalyst properties

Void fraction as macropores = 0.25
Void fraction as micropores = 0.48
Macropore radius = 500nm
Micropore radius = 12nm
Active layer density = 0.5 x 10^{-3} g/mm^3
Rate constant (298 K) = 123.4$mm^3/g \cdot s$
Activation energy = 39,700 J/mol

DESIGN STUDY

Design constraints

A design study for a monolith catalyst section, operating under parameters similar to those listed in Table 1, was performed. For the study, the support wall was assumed to be composed entirely of active catalytic material. Additional constraints, 25% O_2 conversion (Φ_G[exit]=0.75) and a 0.125kPa (≈0.5 in H_20) pressure drop across the monolith section, were imposed. The monolith facial cross sectional area and inlet gas conditions (composition, temperature, flow, and pressure) were held constant. Active support wall thickness and channel opening dimensions were varied and the minimum monolith length determined under the imposed constraint conditions.

The rationale for minimizing the monolith length follows from the assertion that the smallest monolith leads to the smallest, lightest and least expensive laser system. In portable laser systems size, weight, and cost considerations are critical. The choice of the shortest monolith section reduces the system weight by reducing the required monolith section housing length. The housing material weight per unit length is typically an order of magnitude more than that of the monolith material. The monolith material can be quite expensive; a smaller system requires less materials and is less costly. The 25% conversion requirement ensures a constant gas temperature rise. A constant pressure drop across the monolith section ensures that an identical amount of energy is expended to circulate the gas through the system. Excluding laser pulse energy, system energy

requirements (blower energy and heating and cooling loads) are fixed by the pressure drop and conversion requirements. Constant gas inlet conditions and 25% conversion ensure that a chosen laser PRR can be maintained without exceeding a the maximum allowable laser section inlet O_2 concentration.

Design results

Fig. 6 shows the optimum monolith section design geometry in comparison with a standard monolith design. The optimum monolith length is substantially less than the standard monolith length, whereas the optimum support wall thickness is substantially greater than standard thickness. As the monolith support wall thickness is increased, more catalytic material can be packed into a shorter monolith while conversion and pressure drop constraints are still satisfied. However, a thicker support wall has a larger O_2 mass transport resistance. A point is reached where the benefit of having thicker walls is negated by the large O_2 mass transport resistance and an optimum monolith length is determined.

DISCUSSION

The design study presented above shows that the use of off-the-shelf commercial monolith designs for CO_2 laser applications dramatically increases the overall monolith size required relative to the optimum design presented here. Off-the-shelf monoliths are designed for pollutant emission control and have been optimized for large gas flows and fast reactions at high temperatures. They have relatively thin monolith catalyst section dimensions and high % void volume. The slow reaction rates obtained over laser catalysts allow use of relatively thick monolith wall dimensions. With lower gas flow rates, low % void volume can be used to obtain compact monoliths, thereby reducing the size, weight, and cost of the laser system.

Using a computer program to generate variable and parameter values along the length of the monolith allows for rapid optimization of the monolith section under a set of constraints. Use of a computer program also allows for complex channel geometries, such as cylindrical, hexagonal, triangular, etc., to be incorporated into the monolith design.

MODEL IMPLEMENTATION USING LASCAT

LASCAT, a computer program based on the monolith catalyst section model presented above, provides a means to design a monolith catalyst section that will satisfy a user specified set of design requirements. LASCAT is available from the NASA COSMIC Program Office, and the program's order number is LAR-14190. LASCAT requires the specification of the parameters listed in Table 1 and a few others. Values of key parameters (Re, C_{PG}, ρ_g, D_{AB}, D_{ABeff}, and mole fractions) are provided at the inlet and exit of the monolith section. F_G, T and P are integrated instead of the corresponding nondimensional parameters, Φ_G, θ_G and $\wp$. C, T and P values are provided along the length monolith.

See Appendix 1 of this report for information on the implementation and compatibility of LASCAT and Appendix 2 for a short tutorial and an example of the LASCAT output. The documentation supplied with the full program contains an extended tutorial, a detailed explanation of each menu, and a documented program listing.

ACKNOWLEDGEMENT

This work was funded by the NASA Langley Research Center Office of Technology Utilization and Application.

NOTATION

Variables and parameters

A = CO oxidation reaction rate constant (mm^3 / g-cat s)
C = concentration of oxygen (mol / mm^3)
C_{PG} = bulk-average gas heat capacity (J / g K)
D_{AB} = diffusion constant for O_2 in bulk gas mixture (mm^2 / s)
D_{ABeff} = effective diffusion constant for oxygen in porous catalytic layer (mm^2 / s)
d_h = hydraulic diameter of monolith channel, 4(cross sectional area)/(wetted perimeter) (mm)
Eu = Euler number, $Eu = P_0 d_h^4 / \upsilon^2 \rho_g$
F_G = bulk-average gas molar flow rate of oxygen, $F_G = C_G \upsilon$ (mol / s)
h = average heat transfer coefficient (W / mm^2 K)
ΔH_{rxn} = heat of CO oxidation reaction (J / mol O_2 converted)
k = bulk-average gas thermal conductivity (J / m K)
k_m = average mass transfer coefficient (mm / s)
Nu_∞ = limiting Nusselt number, $Nu_\infty = h d_h / k$
P = pressure in the channel at a position ζ (kPa)
$\wp$ = dimensionless pressure at position ζ, $\wp = P / P_0$
Re = Reynolds number , $Re = d_h \upsilon \rho_g / \mu_g d_h^2$
S = Surface area of the channel wall per unit open volume of monolith channel (mm^2/ mm^3)
Sh_∞= limiting Sherwood number, $Sh_\infty = k_m d_h / D_{AB}$
St = Stanton number , $St = h d_h^2 / \upsilon_0 \rho_g C_{PG}$
t_c = characteristic thickness of porous catalytic layer (mm)
T = temperature (K)
x = distance along the length of the monolith channel (mm)
z = depth into the porous catalytic layer (mm)

Subscripts

C,c in porous catalytic layer
G,g in flowing gas
O,o at inlet conditions
W,w in gas at channel wall

Greek

α = dimensionless rate constant, $\alpha = t_c \rho_c \eta A / k_m$
γ = dimensionless mass transfer coefficient, $\gamma = d_h S k_m d_h^2 / \upsilon_0$
Γ = dimensionless volumetric flow rate, $\Gamma = \upsilon / \upsilon_0$
ω = dimensionless heat of reaction, $\omega = -\Delta H_{rxn} k_m F_{G0} / h T_{G0} \upsilon_0$
ζ = dimensionless distance along the length of the monolith channel, $\zeta = x / d_h$
η = effectiveness factor of the reaction in the monolith porous catalytic layer , $\eta = \tanh(\varphi) / \varphi$
θ = dimensionless bulk gas temperature, $\theta_G = T_G / T_{G0}$. $\theta_W = T_W / T_{G0}$
λ = dimensionless depth into the porous catalytic layer, $\lambda = z / t_c$
μ_g = viscosity of gas in channel (Pa-s)
ρ_c = density of porous catalytic layer material (g-cat / mm^3)
ρ_g = density of flowing gas (g / mm^3)
υ = volumetric flow rate of flowing gas (mm^3 / s)
Φ_G = dimensionless bulk-average oxygen concentration in flowing gas, $\Phi_G = F_G / F_{G0}$
Φ_W = dimensionless channel wall surface oxygen concentration, $\Phi_W = [C_W(\zeta)\, \upsilon(\zeta)] / F_{G0}$
φ = Thiele modulus, $\varphi^2 = [t_c^2 \rho_c \eta A] / D_{ABeff}$
Ψ = dimensionless O_2 concentration in the porous catalytic layer. $\Psi(\lambda) = [C_C(\lambda) / C_W(\zeta)]$

REFERENCES

1. Witteman, W. J., The CO_2 Laser, pp. 1-3,22-52,Springer-Verlag, New York (1987).
2. Dudley, W.W., CO_2 Laser, Effects and Applications, pp. 1-12, 36-51, Academic Press, New York, (1976).
3. Upchurch, B.T., G.M. Wood, R.V. Hess, and R.F. Hoyt, "Rare isotope studies involving catalytic oxidation of CO over platinum-tin oxide", in NASA Conference Publication-No.2456, pp.193-197(1987).
4. Stark, D.S., and M.R. Harris, "Catalysed recombination of CO and O_2 in sealed CO_2 TEA laser gases at temperatures down to -27°C", J. Phys. E: Sci. Instrum., (16) 492-496 (1983).
5. Stark, D.S., A. Crocker., and G.J. Steward, "A sealed 100-Hz CO_2 TEA laser using high CO_2 concentrations and ambient-temperature catalysts",J. Phys. E: Sci.Instrum., (16) 158-161 (1983).
6. NASA, Langley Research Center,"Catalytic Oxidation of CO for Closed-Cycle CO_2 Lasers", NASA Tech Briefs, p. 36, June (1987).
7. Price, H.T., and S.R. Shaw, "High repetition rate sealed CO_2 TEA lasers using heterogeneous catalysts", in NASA Conference Publication 2456, pp. 77-84(1987).
8. Burmeister, L.C., Convective Heat Transfer, pp. 240-241, John Wiley and Sons, New York (1983).

Appendix 1: Program Implementation and Compatibility

The LASCAT program is written in the FORTRAN programming language and is compatible with FORTRAN 77 standards. Detailed implementation instructions are provided below for Apple Macintosh and Digital Equipment Corporation VAX computers. Familiarity with the particular operating system is assumed.

Computer: Apple Macintosh SE or II.
Operating System: Apple System Version 6.0
Application Program: Absoft's MacFortran/020 Version 2.3
Compilation Options (Macintosh SE):
-Use compilation options B (Compile Using Long Addresses)
E (Generate Errors List), and
U (* = Unit 9).
Compilation Options (Macintosh II):
-Use compilation options B (Compile Using Long Addresses),
E (Generate Errors List),
M (68020/68030 instructions),
P (68881/68882 instructions), and
U (* = Unit 9).
Compilation and Execution:
-Place the LASCAT program in the same folder as the MacFortran/020 application and supporting files.
-Double click on MacFortran/020 application to launch the MacFortran/020 application.
-From the File Menu choose the "Select File" option. Select File LASCAT.
-From the Compile Menu choose the "Options" option and verify the compilation options selected are identical to the compilation options described above. If the options selected need to be changed, remember to save the new set of compilation options by clicking on the "Save" box. Exit the compilation options section by clicking on the "OK" box.
-From the Compile Menu choose the "Compile and Execute" option. The program will be compiled and executed. The output file, LDATA, and any selectable parameter files will be placed in the same folder as the LASCAT and MacFortran/020 files.

Computer: Digital Equipment Corporation VAX
Operating System: VAX/VMS Version 4.6
Application Program: VAX FORTRAN V4.8-276
Compilation and Execution :
-Rename the LASCAT program *LASCAT.for*
-To compile LASCAT.for, type *for LASCAT.for*
-To link LASCAT.for type *link LASCAT*
-To execute LASCAT.for *type run LASCAT*
-The output file, LDATA.DAT, and any selectable parameter files will be placed in the your directory. Use an editing program to examine files.

NOTE: The FORTRAN program LASCAT is available from the NASA COSMIC Program Office. The program order number is LAR-14190 (1,907 lines)

Appendix 2: LASCAT Tutorial

The LASCAT Tutorial provides a step by step example of the use of the program LASCAT. Required user input and comments are detailed on the left margin and the corresponding screen outputs are indented. Input(s) required by the operater are boldfaced. The example shown below was run on a Macintosh II using Absoft's MacFortran/020 Version 2.3. (Review the Program Implementation and Compatibility section for program complilation and execution details.) This tutorial will be of the greatest benefit if used while actually executing the program.

Compile and execute LASCAT application program.

****** PROGRAM LASCAT *******

The purpose of this program is to calculate the gas concentration and temperature profiles of a monolith catalyst section of a CO2 laser. The CO2 decomposes when the laser is pulsed. The CO and O2 produced as a result of pulsing are detrimental to the efficient operation of the laser. The recombination reaction is CO + 1/2 O2 -> CO. This program provides the means to model the performance of a monolith catalyst section under various gas compositions, temperatures, catalyst activities, gas flowrates, oxygen conversion, monolith face and length dimensions. Results can indicate if constraints such as conversion, maximum gas temperature, and monolith weight are satisfied and how the system parameters may be altered to meet these constraints. Parameters and options may be altered to tailor the monolith design. Default values can also be used as a starting point for the design process. A review of the parameters and options chosen may be made prior to execution of the computational portion of the program.

(HIT RETURN KEY TO CONTINUE)

A program introductory statement is presented. **Hit RETURN key** after reading.

LASCAT Main Menu

1) Read in new operating parameters
2) Show current operating parameters
3) Change operating parameters
4) Run program
5) Exit program

Enter the number corresponding to choice above.

The LASCAT Main Menu is presented. The main menu provides different options (1-5). Specific details for each option are provided in the Menu Description section. To choose one of these options, simply enter the desired number, then RETURN. For this example, **hit the 2 key and hit RETURN key**.

SELECTABLE PARAMETER SUMMARY

Monolith Dimensions(mm):
Support wall thickness: 1.00 Face dimension: 100.00 x 100.00
Channel inner dimension: 4.00 No.Face channels: 20.00 x 20.00
Active layer thickness: .25 % monol.volume open : 64.0

Monolith inlet parameters:
Gas Composition (mole fraction): CO2: .3700 CO: .0200 O2: .0100
N2: .4000 He: .2000 Ar: 0.0000
Gas Flow rate(liters/s): .250 Gas Temperature(K): 300.00
Inlet Gas Pressure (kPa): 101.325

Catalyst Properties:
Catalyst Density (g/mm^3): 0.500E-03
Reaction rate constant at 298K(mm^3 /gcat-s): 123.40
Activation energy(J/mol): 39700.00
Void-fraction as micropores: .24 Void-fraction as macropores: .48
Avg. micropore radius (nm): .12E+02 Avg. macropore radius (nm): .50E+03
Thermal Operation (adiabatic/isothermal): Adiabatic

Computational loop parameters:
Output file (Full Profile/Summary): Full Profile
Termination on (O2 conversion/Length): O2 conversion. %: 2.500
Computation loop step size(mm): .5556 Display every 5.00 mm

==> Hit Return when finished viewing <==

The selectable parameter summary lists the parameter values that will be used in the computation portion of the program. When the program is initially run, default parameter values are assigned. As we'll see later, the values of the parameters can be changed. Hopefully, a review of the parameter summary above will hint to the meaning of each parameter. The use of each parameter is detailed in the Menu Description section. Let's assume the present values are satisfactory and proceed. **Hlit RETURN key.**

LASCAT Main Menu

1) Read in new operating parameters
2) Show current operating parameters
3) Change operating parameters
4) Run program
5) Exit program

Enter the number corresponding to choice above.

We have returned to the main menu. To save space, the main menu will listing will be abbreviated as "LASCAT Main Menu....". To run the computational portion of the program using the current parameter set listed in the selectable parameter summary, **hit 4 key and RETURN key.** Note: the program will alert you that it has completed computations by beeping three times.

*****SEE FILE LDATA FOR RESULTS*****

Initial values

Reynolds number = 9.880
Gas Heat Capacity (J/K-g) = 1.797
Gas Density (g/cm^3) = .0011817
Gas Velocity (mm/s) = 39.063
Effectiveness factor = .99969
Bulk Gas Diffusivity(cm^2/s)= .22540
Effective Diffusivity(cm^2/s)= .053407
Step size(mm) = .555556

Distance mm	%Conver	O2gas mmol/L	O2wall mmol/L	O2center mmol/L	Tgas K	Twall K	DPress kPa
0.000	0.0000	0.4065	0.4060	0.4058	300.000	300.179	-0.0
5.000	0.2239	0.4052	0.4048	0.4046	300.236	300.416	-0.730 E-05
10.000	0.4574	0.4040	0.4035	0.4033	300.474	300.656	-0.146 E-04
15.000	0.6933	0.4027	0.4022	0.4020	300.714	300.897	-0.219 E-04
20.000	0.9314	0.4014	0.4009	0.4008	300.956	301.141	-0.293 E-04
25.000	1.1718	0.4001	0.3996	0.3994	301.201	301.388	-0.366 E-04
30.000	1.4146	0.3988	0.3983	0.3981	301.448	301.637	-0.440 E-04
35.000	1.6598	0.3975	0.3970	0.3968	301.697	301.888	-0.513 E-04
40.000	1.9075	0.3961	0.3957	0.3955	301.949	302.141	-0.587 E-04
45.000	2.1577	0.3948	0.3943	0.3941	302.204	302.398	-0.661 E-04
50.000	2.4104	0.3934	0.3930	0.3928	302.461	302.656	-0.735 E-04
52.778	2.5519	0.3927	0.3922	0.3920	302.605	302.801	-0.776 E-04

Final values

Mole fractions:
He = .2001 Ar = 0.0000 CO2 = .3706
CO = .0195 O2 = .0098 N2 = .4001
Gas Pressure (kPa): 101.325
Reynolds number = 9.817
Gas Heat Capacity (J/K-g) = 1.799
Gas Density (g/cm^3) = .0011720
Gas Velocity (mm/s) = 39.378
Effectivness factor = .99965
Bulk Gas Diffusivity(cm^2/s)= .22832
Effective Diffusivity(cm^2/s)= .053988
Step size(mm) = .555556

==> Hit Return to Return to Main Menu <==

The previous information provides initial and final values of important parameters along with values of key parameters along the length of the monolith. The units for each parameter are specified. A few minutes spent in reviewing the trend of each parameter, either initial vs. final or along the length of the monolith, is well worth the time. For example, the gas heat capacity increases from 1.797 to 1.799 due to the change in gas composition and the change in gas temperature. The gas temperature rises from 300.000 to 302.605 due to the exothermic nature of the reaction $CO + 1/2O_2 \rightarrow CO_2$.

NOTE: The full documentation supplied with LASCAT continues this tutorial.

SECTION III

LABORATORY STUDIES